CHEMISTRY OF MATERIALS

Article

pubs.acs.org/cm

Templated Fabrication of Core–Shell Magnetic Mesoporous Carbon Microspheres in 3-Dimensional Ordered Macroporous Silicas

Minghong Wang,[†] Xiqing Wang,[†] Qin Yue,[†] Yu Zhang,[†] Chun Wang,[†] Jin Chen,[§] Huaqiang Cai,[§] Hongliang Lu,[‡] Ahmed A. Elzatahry,[∥] Dongyuan Zhao,[†] and Yonghui Deng*,[†]

[†]Department of Chemistry, Advanced Materials Laboratory, and State Key Laboratory of Molecular Engineering of Polymers, Fudan University, Shanghai 200433, P. R. China

[‡]State Key Laboratory of ASIC and System, Department of Microelectronics, Fudan University, Shanghai 200433, P. R. China

[§]Institute of Chemical Materials and Advanced Materials Research Center, China Academy of Engineering Physics, Mianyang 621900, Sichuan, P. R. China

[∥]Department of Chemistry-College of Science, King Saud University, Riyadh 11451, Riyadh, Saudi Arabia

Supporting Information

ABSTRACT: A confined synthesis strategy is demonstrated for the fabrication of core–shell magnetic mesoporous carbon microspheres by solvent evaporation induced self-assembly of ethanolic solutions of precursors (containing resol as carbon source, Pluronic F127 as a structure directing agent) in the cavity of presynthesized 3-dimensional ordered macroporous silica materials with each macropore filled with a magnetite particle. The obtained magnetic mesoporous carbon (Fe_3O_4@FDU-15) microspheres possess uniform diameter of ~460 nm, ultralarge mesopores of 13.8 nm, high surface area of ~403 m^2/g, and strong magnetization (20.7 emu/g). Sub-4 nm gold nanoparticles are loaded in the porous shell of the magnetic microspheres, resulting in a novel Fe_3O_4@FDU-15/Au nanocatalyst with an excellent performance in catalyzing the epoxidation of styrene with high conversion (72%) and selectivity (85%) toward styrene oxide in 12 h and a good magnetic field-assisted recyclability.

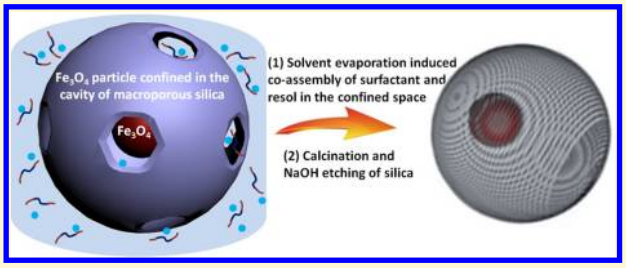

INTRODUCTION

Magnetic nanomaterials have attracted increasing attention due to their unique properties,[1−4] such as superparamagnetism, magnetic separability,[5−9] and the Néel relaxation effect,[10] and, as a result, a broad-range of application in various fields, including magnetic record,[11,12] bioseparation and enrichment,[13,14] catalyst carriers, and hyperthermia treatment.[15−18] Ordered mesoporous carbons (OMCs) have emerged as a family of important nanomaterials due to their uniform pore sizes, excellent biocompatibility, outstanding thermal stability, and chemical inertness. They have also shown great potential applications in separation, catalysis, energy storage/conversion, and drug delivery owing to their high specific surface area, large pore volume, and open porous structure.[19−24] In order to meet various demands, mesoporous carbon materials with different morphologies, including rods,[25,26] fibers,[27,28] tubes,[29,30] thin films,[31,32] and spheres,[33] have been prepared. Among them, monodisperse mesoporous carbon microspheres have drawn particular attention for their good surface permeability and accessibility, low density, and high mechanical stability.[34] Recently, considerable effort has been devoted to synthesizing magnetic mesoporous carbon materials,[35−38] because they combine the properties of magnetic nanomaterials and those of mesoporous carbon materials as mentioned above. They hold a great promise as multifunctional nanomaterials for a variety of applications, such as magnetically guided drug delivery and magnetically recyclable carriers for precious metal catalysts.

The nanocasting method has been widely employed to synthesize magnetic mesoporous carbon materials by introducing both carbon precursors and iron source into the pore channels of mesoporous silica sphere template, followed with *in situ* conversion and subsequent etching away of the hard template, *i.e.* mesoporous silica materials.[35] This strategy usually leads to magnetic iron oxide/carbon composite with ill-defined structure, and the distribution of magnetic component in the composite is usually less controllable. Core–shell structured magnetic mesoporous carbon spheres with magnetic core and porous shell are particularly desired for various applications because of the highly connected porous structure and well-protected magnetic component.[36] In this regards, Fuertes et al.[37] reported magnetic mesoporous carbon spheres with both high mass fraction of magnetic component and high surface area by soaking hollow carbon spheres with disordered mesopores in an ethanol solution of iron nitrate, followed with converting iron ions into iron oxides via thermal treatment

Received: April 3, 2014
Revised: May 1, 2014
Published: May 1, 2014

   dx.doi.org/10.1021/cm501186e | *Chem. Mater.* 2014, 26, 3316−3321

in N_2. The resultant magnetic materials have a magnetic core and mesoporous carbon shell with a thickness of 50 nm and disordered mesopores of 2.0−3.5 nm. By using hollow mesoporous aluminosilicate microspheres as templates, Guo et al.[38] synthesized magnetic core−shell mesoporous carbon microspheres through a two-step nanocasting procedure involving introducing iron nitrate solution into the hollow core of the template and furfuryl alcohol into the mesopores and carbonization and etching the aluminosilicate component. All these nanocasting approaches rely on the presynthesized mesopores and have coherent drawbacks, such as pore blocking, less controlled iron distribution, and ill-defined morphology, which may hamper their applications in various fields.

Recently, a novel confined synthesis method[39,40] has been developed for the creation of monodisperse mesoporous carbon microspheres in three-dimensionally ordered macroporous silica (3DOMS) materials. In this method, an ethanolic precursor solution containing surfactants (e.g., Pluronic F127) and resol is first introduced into the macropores of 3DOMS materials, and after evaporation of solvent, the composite is pyrolyzed in nitrogen and finally subjected to removal of silica by NaOH solution. The obtained ordered mesoporous carbon spheres faithfully replicate the hollow structure of macropores and have uniform size, highly open pore structure, and perfect spherical morphology, which are extremely important and favorable to their applications.

In this study, we extended this synthesis strategy to fabricate magnetic mesoporous carbon microspheres with core−shell structure via a confined fabrication in a novel 3-D ordered macroporous silica (3DOMS) template. First, we synthesized monodisperse core−shell Fe_3O_4@RF resin (resorcinol formaldehyde resin) spheres, which were packed into colloidal crystals. The colloidal crystals were cast with a prehydrolyzed tetraethyl orthosilicate (TEOS) to fill the interstitial voids with amorphous silica. After calcination in air to remove RF, unique magnetic 3DOMS materials with each macropore filled with a magnetic particle were obtained. After that, an ethanolic precursor solution containing template molecules (Pluronic F127) and resol carbon source (i.e., the carbon source) was introduced into the cavities of 3DOMS through continuous evaporation of ethanol. After thermally curing the composite, pyrolysis treatment in N_2 and finally removal silica framework by NaOH etching, magnetic mesoporous carbon microspheres (Fe_3O_4@FDU-15) with a uniform diameter (∼460 nm), large mesopores (∼13.8 nm), and high surface area (∼403 m^2/g) were obtained. By loading sub-4 nm Au nanoparticles into the mesopores of carbon shell, a novel magnetically separable nanocatalyst (Fe_3O_4@FDU-15/Au) was obtained, which exhibited an excellent performance in catalyzing the epoxidation of styrene with high conversion and selectivity toward styrene oxide and good recyclability.

EXPERIMENTAL SECTION

Synthesis of Core−Shell Magnetic Resorcinol-Formaldehyde Resin Microspheres (Denoted as Fe_3O_4@RF). The highly water-dispersible magnetic Fe_3O_4 nanoparticles were synthesized through a solvothermal method as reported before.[14] For a typical preparation, ferric chloride ($FeCl_3{\cdot}6H_2O$, 2.6 g), sodium acetate (NaAc, 4.8 g), and trisodium citrate (1.04 g) were dissolved in ethylene glycol of different volumes (20 mL, 20 mL, and 40 mL) with magnetic stirring, respectively. The obtained transparent solutions were then mixed together and sealed into a Teflon-lined stainless-steel autoclave. The autoclave was heated at 200 °C for 10 h and then allowed to cool down to room temperature. After being washed with deionized water and ethanol several times, the Fe_3O_4 particles were dispersed in 30 mL of ethanol for the next step. The above ethanol solution of Fe_3O_4 nanoparticles (5.0 mL) and concentrated ammonia solution (5.0 mL, 28 wt %) were added to a three-neck round-bottom flask containing a mixed solution of absolute ethanol and deionized water (with total volume of 160 mL, volume ratio:ethanol/H_2O = 2/1) under ultrasonication for 30 min. Afterward, resorcinol (0.8 g) and formaldehyde solution (1.12 mL, 37 wt %) were added under continuous mechanical stirring, and the polymerization reaction was carried out at 35 °C for 12 h. The as-prepared Fe_3O_4@RF microspheres were washed with ethanol 3 times.

Synthesis of Magnetic Silica Inverse Opal (Denoted as Fe_3O_4@3DOMS). The obtained Fe_3O_4@RF microspheres were dispersed in 8 mL of ethanol and sealed for sedimentation for 7 days. After the complete sedimentation, the supernatant liquor was pipetted out, and the wet sediment was dried at 30 °C for 12 h. The brown magnetic opal was then put in an oven at 100 °C for 12 h to consolidate the mechanical stability of the ordered structure of Fe_3O_4@RF microspheres. The obtained opal was allowed to contact and partially soaked in the silica precursor solution containing tetraethyl orthosilicate (TEOS, 2.08 g), hydrochloric acid (2 M, 0.1 g), deionized water (0.9 g), and absolute ethanol (15 g). After drying at 30 °C for 24 h and 70 °C for 6 h, the obtained silica/Fe_3O_4@RF composites were then calcined at 550 °C in air for 5 h with a heating rate of 1 °C/min. Thus, magnetic 3DOMS materials were obtained.

Synthesis of Core−Shell Magnetic Mesoporous Carbon Microspheres (Denoted as Fe_3O_4@FDU-15). The as-synthesized magnetic silica inverse opal (Fe_3O_4@3DOMS) was immersed in a precursor solution containing resol (0.5 g), F127 (0.5 g), and absolute ethanol (5.5 g) at 30 °C. The solvent, ethanol, was allowed to evaporate for 24 h to cause the formation of mesostructured resol/F127 composite shell around the magnetite particles in the macropores. The resulting composite products were heated to 600 °C in nitrogen by a ramp of 1 °C/min and pyrolyzed for 3 h at 600 °C. The obtained Fe_3O_4/carbon/silica composites were finally treated with sodium hydroxide (2 M, 20 mL) at 70 °C for 12 h to remove the silica backbone, and magnetic mesoporous carbon (Fe_3O_4@FDU-15) microspheres were obtained.

Loading Au Nanoparticles. Au nanoparticles were loaded into the mesopores of the core−shell mesoporous Fe_3O_4@FDU-15 microspheres according to the method reported previously.[41] Typically, 50 mg of ethylenediamine (en) was added to the aqueous solution of $HAuCl_4{\cdot}4H_2O$ (0.10 g in 1.0 g of H_2O) until a transparent yellow solution was formed. After stirring for 30 min, 8 mL of ethanol was added to precipitate the $AuCl_3(en)_2$ compound from the solution. The product was filtered, washed with ethanol, and dried in a vacuum oven at 40 °C. 9.0 mg of $AuCl_3(en)_2$ was then dissolved in 10 mL of H_2O, and the pH value of the above solution was adjusted to 10.0 by adding NaOH solution (5.0 wt %). Subsequently, 22 mg of the core−shell mesoporous Fe_3O_4@FDU-15 microsphere was added. After ultrasonication treatment in water bath for 1 h, the sample was separated by a magnet, dried in a vacuum oven at 40 °C for 2 days, and finally reduced by flowing H_2/Ar (5.0%) at 150 °C for 1 h. Thus, magnetic mesoporous carbon microspheres with gold nanoparticles embedded in the mesopores were obtained.

Catalysis. 5.3 mg of Fe_3O_4@FDU-15/Au catalyst was added to a mixture of styrene (1.2 mL, 9 mmol) and acetonitrile (8 mL). The dispersion was bubbled with high-purity Ar for 30 min with magnetic stirring at room temperature. After adding 7.0 g (53 mmol) of *tert*-butyl hydroperoxide (70 wt % in water), the reaction vessel was immersed in an oil bath and heated at 82 °C. During the reaction process, a minor amount of reaction solution (about 20 μL) was carefully withdrawn at different time intervals for gas chromatography−mass spectrometer (GC-MS) measurements. After reaction for 12 h, the reaction system was cooled down, and the catalyst was recycled and washed with acetonitrile 3 times.

Characterization and Measurements. Transmission electron microscopy (TEM) experiments were conducted on a JEOL 2011 microscope (Japan) operated at 200 kV. Field-emission scanning

Scheme 1. Synthesis Strategy of the Magnetic Core−Shell Mesoporous Carbon Microspheres

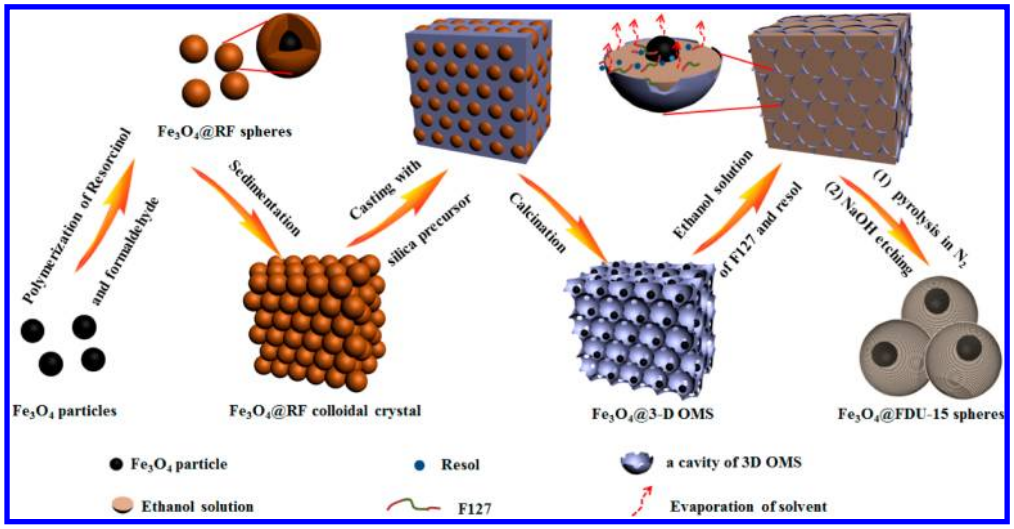

electron microscopy (FESEM) images were collected on the Hitachi Model S-4800 field emission scanning electron microscope. N_2 sorption isotherms were measured at 77 K with a Micromeritics Tristar 3020 analyzer. Before measurements, the samples were degassed in a vacuum at 180 °C for at least 6 h. The Brunauer−Emmett−Teller (BET) method was utilized to calculate the specific surface areas. By using the Barrett−Joyner−Halenda (BJH) model, the pore volumes and pore size distributions were derived from the adsorption branches of isotherms, and the total pore volumes (V_t) were estimated from the adsorbed amount at a relative pressure P/P_0 of 0.995. Wide-angle X-ray diffraction (XRD) patterns were recorded on a Bruker D8 powder X-ray diffractometer (Germany) with Ni-filtered Cu Kα radiation (40 kV, 40 mA). Fourier-transform infrared (FT-IR) spectra were collected on a Nicolet Fourier spectrophotometer using KBr pellets (USA).

■ RESULTS AND DISCUSSION

The synthesis strategy for the core−shell magnetic mesoporous carbon microspheres is depicted in Scheme 1. First, uniform core−shell magnetic microspheres with Fe_3O_4 nanoparticle as the core and resorcinol-formaldehyde (RF) resin as the shell (denoted as Fe_3O_4@RF microspheres) were synthesized and allowed to assemble into a colloidal crystal via gravimetric sedimentation. Second, the obtained colloidal crystals were consolidated by thermal annealing at 100 °C and then were impregnated in an ethanolic solution of prehydrolyzed TEOS as to fill the interstitial voids of colloidal crystals, followed with calcination in air to remove the organic RF resin, resulting in a unique 3-D ordered macroporous silica with each macropore filled with an Fe_3O_4 particle (denoted as Fe_3O_4@3DOMS). Third, the obtained Fe_3O_4@3DOMS materials were immersed in an ethanolic precursor solution containing resol as a carbon source and block copolymer Pluronic F127 as a structure-directing agent (the precursor solution was previously used for synthesis of the ordered mesoporous carbon, FDU-15[42]). After evaporation of ethanol, mesostructured F127-resol composite was incorporated in the macropores of magnetic Fe_3O_4@3DOMS. Finally, the composite was subjected to carbonization and subsequent removal of silica framework by NaOH etching, resulting in magnetic core−shell mesoporous carbon microspheres with Fe_3O_4 nanoparticle as the core and mesoporous carbon as the shell (denoted as Fe_3O_4@FDU-15 microspheres).

Colloidal magnetite particles consisting of nanocrystals were synthesized via the well-established solvothermal method using ethylene glycol as the solvent and reducing agent, ferric chloride as iron source and trisodium citrate as a stabilizer.[12] Due to the stabilization effect of citrate groups capped on the magnetite particles' surface, the colloidal particles (220 nm in diameter) can be well dispersed (Figure 1a). After deposition of

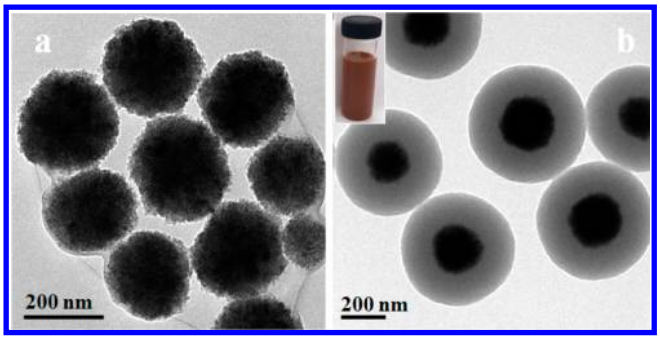

Figure 1. TEM images of (a) the Fe_3O_4 particles synthesized via solvothermal reaction and (b) Fe_3O_4@RF microspheres obtained by coating Fe_3O_4 particles with RF. The inset in part b shows the ethanolic dispersion of Fe_3O_4@RF microspheres (ca. 2 wt %).

a layer of RF resin via the interface polymerization, uniform core−shell structured Fe_3O_4@RF microspheres with a diameter of 520 nm were obtained (Figure 1b). The thickness of the RF shell is about 150 nm. Due to the hydrophilic property of RF resin, the obtained Fe_3O_4@RF microspheres can be readily dispersed in ethanol (Figure 1b, inset), and after sedimentation in ethanol for 1 week, they packed into ordered arrays, forming a 3-D colloidal crystal structure (Figure 2a, b) owing to their uniform size and regular spherical morphology. The as-made 3-D colloidal crystals were further consolidated by annealing at 100 °C and then impregnated in the prehydrolyzed silica precursor solution. The subsequent calcination treatment in air can burn out the organic RF in the composite, giving rise to ordered macroporous silica materials with each cavity filled with an iron oxide particle (Figure 2c, d). SEM observation clearly indicates that the 3-D ordered structure was well retained after removal of RF, due to the good stability of silica framework,

dx.doi.org/10.1021/cm501186e | Chem. Mater. 2014, 26, 3316−3321

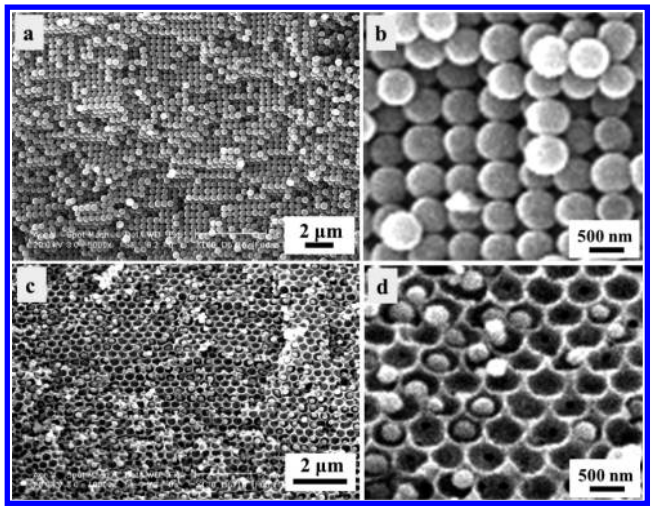

Figure 2. SEM images of (a, b) colloidal crystal arrays of the Fe_3O_4@RF microspheres obtained after sedimentation for 7 days and (c, d) magnetic 3-D ordered macroporous silica obtained after filling the interstitial voids with silica and removal of RF resin by calcination in air.

and the macropores are connected by a large window with size of about 60 nm as marked by the SEM image (Figure 2d).

Transmission electron microscopy image (Figure 3a) reveals that the macropore size is about 500 nm, slightly smaller than

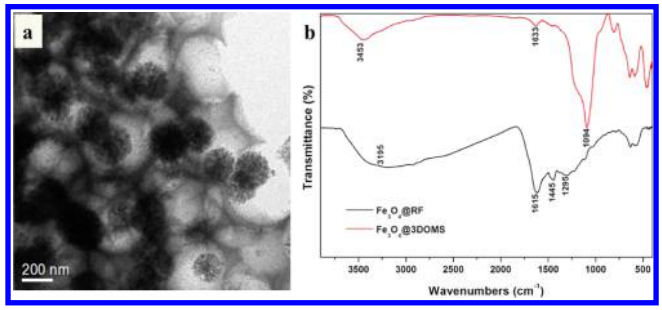

Figure 3. (a) TEM image of the magnetic 3-D ordered macroporous silica (Fe_3O_4@3DOMS) materials and (b) FTIR spectra of Fe_3O_4@RF microspheres and Fe_3O_4@3DOMS.

that of Fe_3O_4 @RF microspheres due to the shrinkage of silica framework during calcination. Magnetite particles were well remained in the macropores with intact spherical morphology; therefore, the Fe_3O_4 particles are separated with each other and thus homogeneously distributed in the matrix of 3-D ordered macroporous silica (3DOMS) materials. Fourier transfer infrared (FTIR) spectrum of the Fe_3O_4@RF microspheres shows adsorption bands at 1615, 1445, and 1295 cm^{-1} which can be assigned to the C═C and C−O stretching of resorcinol-formaldehyde resin, respectively, while magnetic 3DOMS materials show that these bands are nearly indiscernible, suggesting the efficient removal of the RF resin. The absorption peaks at 1094 cm^{-1} can attribute to the Si−O−Si stretching of silica.

Upon contact with the ethanolic precursor solution (usually for synthesis of mesoporous carbon, FDU-15) containing resol and Pluronic F127 template molecules, the macropores of this novel magnetic 3DOMS materials can be easily filled with phenolic resin/F127 composite after evaporation of ethanol. After thermosetting treatment, carbonization and removing silica framework by a hot NaOH solution, core−shell structured magnetic mesoporous carbon microspheres (Fe_3O_4@FDU-15) were obtained. The TEM image indicates that magnetite particles were individually coated by mesoporous carbon shells (Figure 4a). Notably, most of the obtained

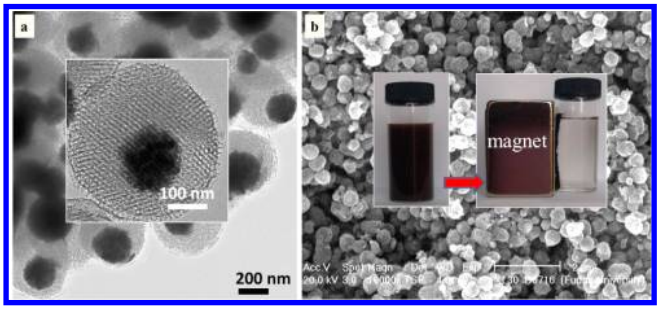

Figure 4. TEM (a) and SEM (b) image of Fe_3O_4@FDU-15 microspheres. The insets show the magnified TEM image (a) and magnetic separation process of Fe_3O_4@FDU-15 microspheres (b).

microspheres have an eccentric structure, which is probably caused by the gravity effect and magnetic dipolar interaction during gradual coating by PF/F127 composite with ethanol evaporation under static conditions. Moreover, the magnified TEM image (Figure 4a, inset) reveals the ordered array of mesopore channels with 2-D hexagonal arrangement in the carbon shell. The SEM image shows that the obtained Fe_3O_4@FDU-15 materials are nearly spherical in morphology, in agreement with the TEM image (Figure 4a). They have a mean diameter of about 460 nm (Figure 4b), which is smaller than the cavity size (ca. 500 nm). It accounts for a shrinkage of about 22% caused by the removal of F127 and carbonization of PF during pyrolysis treatment. With an ultrasonication treatment for 2 min (40 kHz, 600 W), the microspheres can be readily dispersed in water solution (Figure 4b, inset) and separated from the resultant homogeneous solution with a magnet (4000 Oe) within 30 s, which indicates a good magnetic responsiveness of the microspheres.

Nitrogen adsorption−desorption isotherms of the obtained Fe_3O_4@FDU-15 microspheres (Figure S1A) exhibit a type IV curve with a sharp capillary condensation step in the P/P_0 range of 0.8−0.9, implying a uniform and large mesopore. The Brunauer−Emmett−Teller (BET) specific surface area and a total pore volume were calculated to be of 403 m^2/g and 0.66 cm^3/g, respectively. The pore-size distribution curve (Figure S1B) calculated using the Barrett−Joyner−Halenda (BJH) method reveals a large pore size of 13.8 nm. This value is much larger than that (around 4.0 nm) of the mesoporous carbon materials (FDU-15) previously reported, which are usually synthesized via carbonization of mesostructured PF/F127 composite in N_2 without protection. While for Fe_3O_4@FDU-15 microspheres, although the carbonization temperature for Fe_3O_4@3DOMS-PF/F127 composite is similar, the shrinkage is much smaller than typical FDU-15 (about 40%)[42] due to the protection and the supporting effect of the rigid silica walls of 3DOMS and magnetite particles in the cavities. Therefore, this novel confined synthesis in macroporous silica materials is favorable for creation of large-pore mesoporous carbon. X-ray diffraction measurements indicate that Fe_3O_4 particles and Fe_3O_4@FDU-15 microspheres (Figure S2) have similar diffraction peaks, typical for the Fe_3O_4 crystalline phase; however, the diffraction peaks for the Fe_3O_4@FDU-15

dx.doi.org/10.1021/cm501186e | Chem. Mater. 2014, 26, 3316−3321

microspheres are slightly sharper than those of the Fe_3O_4 particles, implying the growth of nanocrystals in the magnetite particles during high-temperature treatment. Calculations with the Debye–Scherrer formula for the most intense (311) diffraction peak indicate that the grain size significantly increases from 10.2 nm for initial Fe_3O_4 particles to 14.8 nm for Fe_3O_4@FDU-15 microspheres.

Since the obtained Fe_3O_4@FDU-15 microspheres have unique magnetic responsivity, and stable mesoporous carbon shell, they hold a great promise for many applications, such as catalysis, separation, drug delivery, and sensing. In this study, in order to investigate the feasibility for application in catalysis, ultrafine Au nanoparticles were loaded in the mesopores of Fe_3O_4@FDU-15 microspheres via the *in situ* reduction method for the use as a novel nanocatalyst for styrene epoxidation at 82 °C using *tert*-butylhydroperoxide (TBHP) as an oxidant under argon atmosphere. TEM observation shows that the obtained Fe_3O_4@FDU-15/Au microspheres maintain their ordered mesoporous structure (Figure 5), and Au nanoparticles with

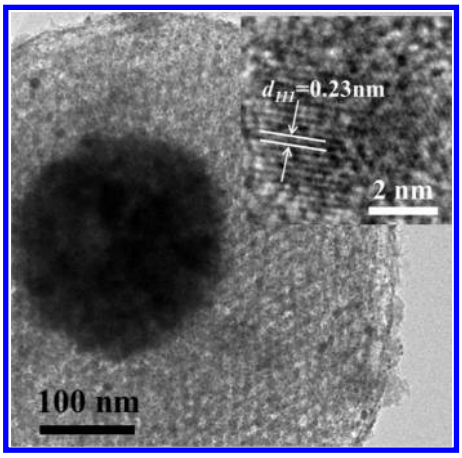

Figure 5. TEM images of Fe_3O_4@FDU-15/Au obtained by deposition of Au nanoparticles in the mesopores of a mesoporous carbon shell via an in situ reduction method. The inset is the high-resolution TEM image of Au nanoparticle.

a diameter of about 4.0 nm are highly dispersed in the mesopores. The high-resolution TEM image clearly shows the lattice fringes of the crystalline Au nanoparticles (Figure 5, inset). In the wide-angle XRD patterns of the Fe_3O_4@FDU-15/Au nanocatalysts, besides the diffraction peaks from magnetite particles, typical broadened diffraction peaks attributed to the *fcc*-structured Au nanoparticles were also detected (Figure S3). The specific surface area of the Au loaded samples (Fe_3O_4@FDU-15/Au) decrease to 290 m^2/g, while the total pore volume and pore size reduce to 0.54 cm^3/g (P/P_0 = 0.99) and 12.4 nm, respectively (Figure S4).

The loading amount of Au nanoparticles was measured to be about 1.2 wt % by inductively coupled plasma-atomic emission spectrometry (ICP-AES). The room-temperature magnetic characterization using a magnetometer at 300 K indicates that the Fe_3O_4@FDU-15/Au microspheres possess ferromagnetic property and high magnetization saturation value of 20.7 emu/g (Figure S5). The remanence and coercivity are calculated to be as low as 1.7 $emug^{-1}$ and 80 Oe, respectively. Therefore, this nanocatalyst can be easily recycled with a magnet and redispersed in liquid solutions for catalysis. The catalytic results of styrene epoxidation were summarized in Figure 6. It

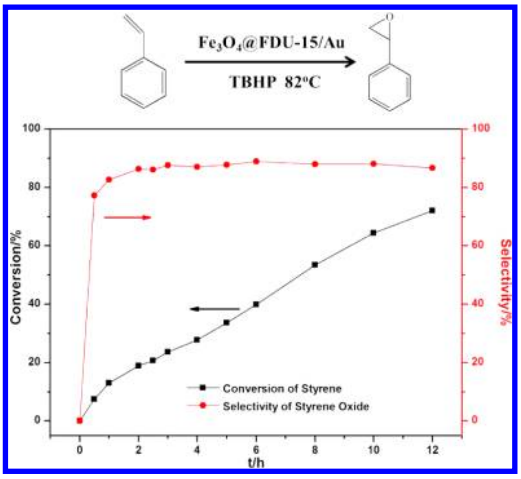

Figure 6. The conversion of styrene and the selectivity toward styrene oxide at different reaction time.

can be seen that the conversion of styrene increases with the reaction time linearly and reaches 72% at 12 h, and the selectivity toward styrene oxide quickly reaches 85% in 2 h and becomes stabilized in the subsequent 10 h. Compared with the previously reported Fe_3O_4@SiO_2–Au@mSiO_2 catalysts,[43] the selectivity toward styrene oxide is more stable and the reaction rate is more quick. It is speculated that, such a good selectivity is related with the highly accessible, uniform large mesopores of the Fe_3O_4@FDU-15/Au microspheres, which facilitates the molecules to diffuse and contact Au nanoparticles. Additionally, the carbonaceous porous shell favors the enrichment of reactants and thus contributes to a quick reaction rate of styrene. Notably, the Fe_3O_4@FDU-15/Au microspheres can be recycled with an applied magnetic field without reduction of performance in practical applications even after use for more than 10 times.

CONCLUSIONS

In summary, a confined synthesis strategy has been demonstrated for creation of the core–shell magnetic mesoporous carbon (Fe_3O_4@FDU-15) microspheres through the solvent evaporation-induced self-assembly process in magnetic three-dimensionally ordered macroporous silica (Fe_3O_4@3DOMS) materials. By using the core–shell magnetic resorcinol-formaldehyde resin microspheres (Fe_3O_4@RF) as the building block for assembly of colloidal crystals, the novel Fe_3O_4@3DOMS materials with each macropore filled with a magnetite particle can be obtained after replicating by silica. Since the size is determined by the diameter of original core–shell Fe_3O_4@RF spheres, the particle size of the obtained Fe_3O_4@FDU-15 spheres can be easily controlled by changing the magnetic particle size and the polymer shell thickness of Fe_3O_4@RF. The synthesized core–shell magnetic mesoporous carbon microspheres show high specific surface areas (~403 m^2/g) and large pore size (~13.8 nm). By use of the large mesopores, Au nanoparticles (~4 nm) were successfully loaded in the carbon shell, and the obtained Fe_3O_4@FDU-15/Au nanocatalyst exhibits an excellent performance in catalyzing the epoxidation of styrene with high conversion (72%) and selectivity (85%) toward styrene oxide in 12 h and good recyclability. Considering the versatility of this synthesis method, other core–shell microspheres with various functional

dx.doi.org/10.1021/cm501186e | *Chem. Mater.* 2014, 26, 3316–3321

cores and porous or nonporous shell of diverse compositions can be fabricated using this method.

■ ASSOCIATED CONTENT

Supporting Information

Nitrogen adsorption−desorption isotherms of Fe_3O_4@FDU-15 and Fe_3O_4@FDU-15/Au microspheres. XRD patterns of Fe_3O_4, Fe_3O_4@FDU-15, and Fe_3O_4@FDU-15/Au microspheres. The magnetic hysteresis loop of Fe_3O_4@FDU-15/Au microspheres. This material is available free of charge via the Internet at http://pubs.acs.org.

■ AUTHOR INFORMATION

Corresponding Author

*E-mail: yhdeng@fudan.edu.cn.

Notes

The authors declare no competing financial interest.

■ ACKNOWLEDGMENTS

This work was supported by the State Key 973 Program of PRC (2013CB934104 and 2012CB224805), the NSF of China (51372041, 51102048, and 61376008), the specialized research fund for the doctoral program of higher education of China (20120071110007, 20110071120017), the innovation program of Shanghai Municipal Education Commission (13ZZ004), Shanghai Rising Star Project of STCSM (12QH1400300), Program for New Century Excellent Talents in University (NCET-12-0123), and the "'Shu Guang'" Project (13SG02) supported by Shanghai Municipal Education Commission and Shanghai Education Development Foundation. The authors extend their appreciation to the Deanship of Scientific Research at King Saud University for funding the work through the research group project No. RGP-VPP-036.

■ REFERENCES

(1) Ferrari, M. *Nat. Rev. Cancer* **2005**, *5*, 161−171.

(2) Hahn, Y. K.; Jin, Z.; Kang, H.; Oh, E.; Han, M.-K.; Kim, H.-S.; Jang, J.-T.; Lee, J. H.; Cheon, J.; Kim, S. H.; Park, J. K. *Anal. Chem.* **2007**, *79*, 2214−2220.

(3) Zhang, L.; Qiao, S. Z.; Jin, Y. G.; Chen, Z. G.; Gu, H. C.; Lu, G. Q. *Adv. Mater.* **2008**, *20*, 805−809.

(4) Liu, J.; Qiao, S. Z.; Hu, Q. H.; Lu, G. Q. *Small* **2011**, *7*, 425−443.

(5) Lou, X. W.; Archer, L. A. *Adv. Mater.* **2008**, *20*, 1853−1858.

(6) Zhang, L.; Qiao, S. Z.; Jin, Y. G.; Yang, H. G.; Budihartono, S.; Stahr, F.; Yan, Z. F.; Wang, X. L.; Hao, Z. P.; Lu, G. Q. *Adv. Funct. Mater.* **2008**, *18*, 3203−3212.

(7) Weissleder, R.; Moore, A.; Mahmood, U.; Bhorada, R.; Benveniste, H.; Chiocca, E. A.; Basilion, J. P. *Nat. Med.* **2000**, *6*, 351−354.

(8) Zhang, L.; Qiao, S. Z.; Cheng, L. N.; Yan, Z. F.; Lu, G. Q. *Nanotechnology* **2008**, *19*, 435608.

(9) Wang, M. H.; Sun, Z. K.; Yue, Q.; Yang, J.; Wang, X. Q.; Deng, Y. H.; Yu, C. Z.; Zhao, D. Y. *J. Am. Chem. Soc.* **2014**, *136*, 1884−1892.

(10) Park, J. H.; Derfus, A. M.; Segal, E.; Vecchio, K. S.; Bhatia, S. N.; Sailor, M. J. *J. Am. Chem. Soc.* **2006**, *128*, 7938−7946.

(11) Jordan, A.; Scholz, R.; Wust, P.; Fahling, H.; Felix, R. *J. Magn. Magn. Mater.* **1999**, *201*, 413−419.

(12) Jun, Y. W.; Huh, Y. M.; Choi, J. S.; Lee, J. H.; Song, H. T.; Kim, S.; Yoon, S.; Kim, K. S.; Shin, J. S.; Suh, J. S.; Cheon, J. *J. Am. Chem. Soc.* **2005**, *127*, 5732−5733.

(13) Deng, Y. H.; Qi, D. W.; Deng, C. H.; Zhang, X. M.; Zhao, D. Y. *J. Am. Chem. Soc.* **2008**, *130*, 28−29.

(14) Liu, J.; Sun, Z. K.; Deng, Y. H.; Zou, Y.; Li, C. Y.; Guo, X. H.; Xiong, L. Q.; Gao, Y.; Li, F. Y.; Zhao, D. Y. *Angew. Chem., Int. Ed.* **2009**, *48*, 5875−5879.

(15) Lewin, M.; Carlesso, N.; Tung, C. H.; Tang, X. W.; Cory, D.; Scadden, D. T.; Weissleder, R. *Nat. Biotechnol.* **2000**, *18*, 410−414.

(16) Son, S. J.; Reichel, J.; He, B.; Schuchman, M.; Lee, S. B. *J. Am. Chem. Soc.* **2005**, *127*, 7316−7317.

(17) Rosi, N.; Mirkin, C. A. *Chem. Rev.* **2005**, *105*, 1547−1562.

(18) Kim, J.; Park, S.; Lee, J. E.; Jin, S. M.; Lee, J. H.; Yang, I.; Kim, J. S.; Kim, S. K.; Cho, M. H.; Hyeon, T. *Angew. Chem., Int. Ed.* **2006**, *45*, 7754−7758.

(19) Ryoo, R.; Joo, S.; Jun, S. *J. Phys. Chem. B* **1999**, *103*, 7743−7746.

(20) Jun, S.; Joo, S.; Ryoo, R.; Kruk, M.; Jaroniec, M.; Liu, Z.; Obsuna, T.; Terasaki, O. *J. Am. Chem. Soc.* **2000**, *122*, 10712−10713.

(21) Joo, S.; Choi, S.; Oh, I.; Kwak, J.; Liu, Z.; Terasaki, O.; Ryoo, R. *Nature* **2001**, *412*, 169−172.

(22) Fan, J.; Yu, C.; Gao, F.; Lei, J.; Tian, B.; Wang, L.; Lu, Q.; Tu, B.; Zhou, W.; Zhao, D. *Angew. Chem., Int. Ed.* **2003**, *115*, 3254−3258.

(23) Liang, C.; Li, Z.; Dai, S. *Angew. Chem., Int. Ed.* **2008**, *120*, 3754−3776.

(24) Xia, K.; Gao, Q.; Jiang, J.; Hu, J. *Carbon* **2008**, *46*, 1718−1726.

(25) Yu, C. Z.; Fan, J.; Tian, B. Z.; Zhao, D. Y.; Stucky, G. D. *Adv. Mater.* **2002**, *14*, 1742−1745.

(26) Xia, Y. D.; Yang, Z. X.; Mokaya, R. *Chem. Mater.* **2006**, *18*, 140−148.

(27) Tamai, H.; Yoshida, T.; Sasaki, M.; Yasuda, H. *Carbon* **1999**, *37*, 983−989.

(28) Wang, K.; Birjukovs, P.; Erts, D.; Phelan, R.; Morris, M. A.; Zhou, H.; Holmes, J. D. *J. Mater. Chem.* **2009**, *19*, 1331−1338.

(29) Minsuk, K.; Kwonnam, S.; Jaeyun, K.; Taeghwan, H. *Chem. Commun.* **2003**, 652−653.

(30) Chen, X. C.; Cendrowski, K.; Nazzal, J. S.; Rümmeli, M.; Kalenczuk, R. J.; Chen, H.; Chu, P. K.; Palen, E. B. *Colloids Surf., A* **2011**, *377*, 150−155.

(31) Feng, D.; Lv, Y. Y.; Wu, Z. X.; Dou, Y. Q.; Han, L.; Sun, Z. K.; Xia, Y. Y.; Zheng, G. F.; Zhao, D. Y. *J. Am. Chem. Soc.* **2011**, *133*, 15148−15156.

(32) Dai, M. Z.; Song, L. Y.; LaBlle, J. T.; Vogt, B. D. *Chem. Mater.* **2011**, *23*, 2869−2878.

(33) Zhou, J. H.; He, J. P.; Zhang, C. X.; Wang, T.; Sun, D.; Di, Z. Y.; Wang, D. *J. Mater. Charact.* **2010**, *61*, 31−38.

(34) Fang, Y.; Gu, D.; Zou, Y.; Wu, Z. X.; Li, F. Y.; Che, R. C.; Deng, Y. H.; Tu, B.; Zhao, D. Y. *Angew. Chem., Int. Ed.* **2010**, *49*, 7987−7991.

(35) Dong, X. P.; Chen, H. R.; Zhao, W. R.; Li, X.; Shi, J. L. *Chem. Mater.* **2007**, *19*, 3484−3490.

(36) Yin, Y. Y.; Zhou, S. X.; Min, C.; Wu, L. M. *J. Colloid Interface Sci.* **2011**, *361*, 527−533.

(37) Fuertes, A. B.; Sevilla, M.; Valdes-Solis, T.; Tartaj, P. *Chem. Mater.* **2007**, *19*, 5418−5423.

(38) Guo, L. M.; Cui, X. Z.; Li, Y. S.; He, Q. J.; Zhang, L. X.; Bu, W. B.; Shi, J. L. *Chem.—Asian J.* **2009**, *4*, 1480−1485.

(39) Schuster, J.; He, G.; Mandlmeier, B.; Yim, T.; Lee, K. T.; Bein, T.; Nazar, L. F. *Angew. Chem., Int. Ed.* **2012**, *51*, 3591−3595.

(40) Sun, Z. K.; Liu, Y.; Li, B.; Wei, J.; Wang, M. H.; Yue, Q.; Deng, Y. H.; Kaliaguine, S.; Zhao, D. Y. *ACS Nano* **2013**, *7*, 8706−8714.

(41) Zhu, H. G.; Liang, C. D.; Yan, W. F.; Overbury, S. H.; Dai, S. *J. Phys. Chem. B* **2006**, *110*, 10842−10848.

(42) Meng, Y.; Gu, D.; Zhang, F. Q.; Shi, Y. F.; Yang, H. F.; Li, Z.; Yu, C. Z.; Tu, B.; Zhao, D. Y. *Angew. Chem., Int. Ed.* **2005**, *44*, 7053−7059.

(43) Deng, Y. H.; Cai, Y.; Sun, Z. K.; Liu, J.; Liu, C.; Wei, J.; Li, W.; Liu, C.; Wang, Y.; Zhao, D. Y. *J. Am. Chem. Soc.* **2010**, *132*, 8466−8473.